PERGAMON

International Journal of Multiphase Flow 27 (2001) 843–859

International Journal of Multiphase Flow

www.elsevier.com/locate/ijmulflow

Drop size distributions in dispersed liquid–liquid pipe flow

M.J.H. Simmons *, B.J. Azzopardi

School of Chemical, Environmental and Mining Engineering, University of Nottingham, Nottingham, NG7 2RD, UK

Received 10 January 2000; received in revised form 9 September 2000

Abstract

This paper examines drop size distributions in a 0.063 m pipe for a two-phase mixture of kerosene and aqueous potassium carbonate solution. Measurements have been made for both vertical upflow and horizontal geometries, for mixture velocities ranging from 0.8 to 3.1 m/s.

Two optical measurement techniques, a backscatter technique using a Par-Tec 300C and a diffraction technique using a Malvern 2600, have been used to obtain the drop size distributions of the dispersions created. Both measurement techniques have been found to be limited to different concentration ranges. Stratification of drop size was observed for low mixture velocities in a horizontal geometry. This did not occur for the vertical geometry.

The drop distributions obtained were found to fit an upper limit log-normal distribution (ULLN). The theory of Hinze has been found to agree well with experimentally determined values of maximum drop diameter at low dispersed phase concentrations. At high concentrations, neither Hinze theory, nor a modified version proposed previously, adequately describe the data obtained.

1. Introduction

The majority of studies of drop sizes in multiphase flow have been carried out for two-phase gas-liquid systems, most typically for flows of air and water. However, two-phase systems in the oil, chemical and food industries can consist of dispersions of two immiscible liquids, and the literature available is rather limited by comparison. The size distribution of these dispersed droplets is important because it has a very significant effect upon equipment performance, for example, in liquid–liquid contactors or phase separators.

* Corresponding author. Present address: School of Chemical Engineering, University of Birmingham, Edgbaston, Birmingham B15 2TT, UK. Tel.: +121-414-5321; fax: +121-414-5324.

E-mail address: m.j.simmons@bham.ac.uk (M.J.H. Simmons).

0301-9322/01/$ - see front matter
PII: S0301-9322(00)00055-0

There are significant differences between the flow patterns that occur for gas–liquid and liquid–liquid systems. The density ratio of the fluids is typically in the range of 0.7–1.1, compared with values lower than 0.001–0.2 for gas–liquid systems. Additionally, a wide range of viscosity ratios is possible depending on the type of oil being used. This means it is much more difficult to draw general conclusions about the behaviour of liquid–liquid systems compared to gas–liquid systems. Any droplets formed by shear between the two phases will remain suspended in the flow, unless the settling of the drops by gravitational forces can overcome the turbulence within the continuous phase. For liquid–liquid systems, the continuous phase is much denser and more viscous than for a gas–liquid system, so the settling of droplets occurs much less rapidly. Therefore there is a greater propensity to form a dispersion.

In spite of the importance and prevalence of dispersions in liquid–liquid pipe flows, there have only been a small number of studies in which drop size distributions have been measured. The sources, geometry, physical properties and measurement techniques employed are listed in Table 1. A wide variety of measurement techniques have been employed. El-Hamouz et al. (1995) utilised a laser diffraction technique (Malvern 2600) whilst El-Hamouz and Stewart (1996) also employed a laser backscatter technique (Par-Tec M300 instrument). Kubie and Gardner (1977), Angeli and Hewitt (2000) and Kurban et al. (1995) have used photographic techniques. The latter also used needle conductivity probes to measure local drop size and found significant differences between the two results. Sauter mean diameters of 678 μm for the photographic technique and 206 μm for the conductivity technique were reported at the same flow conditions. Karabelas (1978) used a totally different approach whereby the droplets were encapsulated using a polymer so the particle size distribution remained constant. A feature of these data is that they have all been obtained for low concentrations of the dispersed phase. Su and Hanzevack (1988) used a laser image processing technique to determine the sizes of water droplets injected into a continuously flowing oil phase in pipes of different diameter. However, they did not find as large a fraction of small droplets as other workers, e.g., Kurban et al. (1995). All these experiments have been performed at relatively low concentrations of the dispersed phase and there is a paucity of drop size data for concentrated dispersions.

As a preliminary to measuring drop size distributions, it is necessary to know at which flow conditions dispersions will occur. Flow pattern classifications available in the literature have been based upon visual observations of liquids flowing in transparent tubes. Previous work in this area has been reviewed extensively by Valle (1998). Recently, Trallero (1995) classified flow pattern, and measured pressure drop and hold-up mixtures of water and different oils in a 0.051 m pipe. Angeli and Hewitt (2000) studied the effect of tube material and obtained flow patterns, drop size, pressure drop and hold-up in 0.0254 m acrylic and steel pipes.

This paper describes measurements of drop size for a mixture of potassium carbonate solution dispersed in kerosene, flowing in a 0.063 m pipe. Measurements have been made for horizontal flow and vertical upflow using two optical techniques. A Lasentec™ Par-Tec 300C instrument has been used for measurements at high concentrations of the dispersed phase, and a Malvern 2600 particle size analyser has been used at low concentrations. The accuracy of the techniques was checked by simultaneous measurement of glass beads suspended in water within a test cell for which details appear in Simmons et al. (1999). The drop distributions obtained have been found to fit an upper limit log-normal distribution function. Prediction of the maximum drop size for the low concentration data in this study, and for previous studies, can be well predicted by the

Table 1
Sources of liquid/liquid drop size data compared to present study

	Author	Pipe diameter (m)	Interfacial tension (N/m)	Oil viscosity (kg/ms)	Oil density $(kg/m)^3$	Dispersed phase conc. (%vol)	Dispersion	Measurement technique
A	El-Hamouz and Stewart	0.025	0.038	0.00096	800	1	o/w	Malvern 2600 and Par-Tec M300
B	Karabelas (w/to)	0.05	0.033	0.018	890	< 1	w/o	Photography of encapsulated sampled drops
C	Karabelas (w/k)	0.05	0.03	0.00186	808	< 1		
D	Kubie and Gardner (water/alcohol)	0.017	0.0049	0.0048	828	< 1	w/o and o/w	Photography of drops inside pipe
E	Kubie and Gardner (water/acetate)	0.017	0.0145	0.0007	884	< 1		
F	Kurban et al.	0.025	0.017	0.0016	800	3.4–9.1	w/o	Photography using borescope plus conductivity probe
	Angeli and Hewitt (2000)	0.025	0.017	0.0016	800	3.4–9.1	w/o	Photography using borescope plus conductivity probe
	Su and Hanzevack (1988)	0.0508, 0.0762, 0.1016	n/a	0.0014–0.0023	800	n/a	w/o	Laser image processing
G	Vertical flow	0.063	0.01	0.0018	797	1.2–3.3 (low); 6–42 (high)	w/o	Malvern 2600 and Par-Tec 300C
H	Horizontal flow	0.063	0.01	0.0018	797	6–42		

analysis of Hinze (1955). However, the data obtained at high concentrations does not agree with this analysis, or an analysis modified to include drop coalescence, proposed by Brauner (1999).

Flow patterns have been identified from high-speed video footage and compared with the flow map of Trallero (1995). Stratified flows and dispersions were obtained for the horizontal geometry. For vertical upflow, dispersions of the aqueous phase in kerosene were obtained.

2. Theory

2.1. Modelling of drop size distribution

Prediction of droplet size distribution requires use of a distribution function. Karabelas (1978) applied the Rosin–Rammler distribution function (Rosin and Rammler, 1933) and the upper-limit-log normal distribution, described by Mugele and Evans (1951), to experimental data obtained from pipe flows of water droplets dispersed in either kerosene or a viscous oil. Recently Angeli and Hewitt (2000) used the Rosin–Rammler distribution exclusively. A disadvantage of the Rosin–Rammler distribution is that it does not contain a mathematical upper cut-off, it has a tail to infinite drop sizes. It can be argued that this is against physical reasonableness so in these studies the upper-limit log-normal function was used.

$$f(d) = 1 - \frac{1}{2}[1 - \mathrm{erf}(\delta z)], \tag{1}$$

where the cumulative volume fraction of particles smaller than size d is $f(d)$, and

$$z = \ln\left[\frac{ad}{d_{\max} - d}\right], \tag{2}$$

$$a = \frac{d_{\max} - d_{50}}{d_{50}}, \tag{3}$$

$$\frac{d_{\max}}{d_{50}} = \frac{d_{50}(d_{90} + d_{10}) - 2d_{90}d_{10}}{d_{50}^2 - d_{90}d_{10}} \tag{4}$$

and

$$\delta = \frac{0.394}{\log_{10}\left[\frac{v_{90}}{v_{10}}\right]}, \tag{5}$$

where the maximum drop diameter is $d_{\max}$, the diameter for which i% of the drops are smaller is d_i, and $v_i = d_i/(d_{\max} - d_i)$. The adjustable parameters in the distribution are a and δ, which can be obtained from the experimental data. Values of $a = 1.2$ and $\delta = 0.9$ were determined by Karabelas for kerosene–water dispersions. This distribution can be normalised, following the approach of Pacek and Nienow (1997), by dividing through by the Sauter mean diameter, i.e. $X = d/d_{32}$, and

$$d_{32} = \frac{\sum d^3 n(d)}{\sum d^2 n(d)}, \tag{6}$$

where n is the number of drops of size d.

A theoretical determination of d_{max} can be made by considering the emulsification of a dispersed phase in a turbulent flow field. Most of the models for predicting maximum drop size are based on the model of Hinze (1955).

$$\frac{(d_{max})_0}{D} = 0.55\left(\frac{\rho_c u_c^2 D}{\sigma}\right)^{-0.6} f^{-0.4}, \tag{7}$$

where the velocity of the continuous phase is u_c, the density of the continuous phase is ρ_c, the interfacial tension is σ, and the pipe diameter is D.

The friction factor, f, can be calculated for a smooth conduit from the Blasius equation,

$$f = \frac{0.046}{Re_c^{0.2}}. \tag{8}$$

This analysis was derived by considering a single drop in an infinite flow field. This is only valid in a dilute flow field, where droplet coalescence does not occur. In concentrated flows, Brauner (1999) argued that the incoming flow of the continuous phase should carry enough turbulent energy to disrupt the coalescence of the dispersed phase. This energy balance led to the relationship below.

$$\frac{(d_{max})_\varepsilon}{D} = 7.6 C_H^{0.6} We_c^{-0.6} Re_c^{0.08} \left(\frac{\rho_c}{\rho_m}\right)^{0.4} \left(\frac{\varepsilon_d^{0.6}}{(1-\varepsilon_d)^{0.2}}\right), \tag{9}$$

where the density of the mixture is ρ_m, and the void fraction of the dispersed phase is ϵ_d, defined as

$$\varepsilon_d = \frac{u_{sd}}{u_{sd} + u_{sc}}, \quad u_c = u_d = u_{sd} + u_{sc} \equiv u_m \tag{10}$$

and

$$We_c = \frac{\rho_c u_c^2 D}{\sigma}, \quad Re_c = \frac{\rho_c u_c D}{\eta_c}. \tag{11}$$

where the continuous phase dynamic viscosity is η_c.

Accurate experimental determination of d_{max} is difficult because it is dependent on the number of droplets sampled. Azzopardi and Hibberd (1994) showed that normalised values of d_{max}, determined from experimental data, tended to increase with droplet sample size at the same flow conditions. This is particularly noticeable for photographic sizing techniques, because the difficulty in obtaining good quality photographs has caused the sample size to be small. The optical techniques used in this study cannot be used directly to obtain d_{max} because each technique has an upper size limit, but the number of drops sampled by each instrument is very large. If the distribution is fitted to the upper-limit log normal function, a value of d_{max} can be inferred from the Sauter mean diameter.

$$d_{32} = \frac{d_{\max}}{1 + a \exp\left(\frac{1}{4\delta^2}\right)}. \tag{12}$$

2.2. Flow pattern transitions

The generation of a unified theory for the prediction of flow pattern for liquid–liquid flows is not possible due to the wide variation of physical properties and surface chemistry of different oils. Some oils can also exhibit non-Newtonian behaviour, which further complicates the analysis. However, some general guidelines have been presented, based on the linear stability analysis of a stratified flow (Milne-Thomson, 1968), and various different mechanisms to define the transition to dispersed flow. Trallero (1995) and Brauner and Moalem Maron (1992a,b) have proposed generalised flow pattern maps for liquid–liquid systems. These were optimised for low viscosity oils and high viscosity oils, respectively, and Valle (1998) discusses the differences between them. The experiments performed in this work were made using low viscosity oil, so the flow patterns observed are compared to the flow map of Trallero (1995).

3. Experiments

3.1. Flow facility

A schematic of the flow facility is shown in Fig. 1. The facility was operated with kerosene (continuous phase) and 25% by weight potassium carbonate solution (dispersed phase). The physical properties of the phases are given in Table 2. Potassium carbonate was used to increase the density of the aqueous phase to values experienced in oil–water pipelines due to the presence of salts. The pipe diameter used was 63 mm and both vertical and horizontal test sections were used. The two liquids were pumped from their respective storage tanks and orifice plates metered their flow rates. The liquids were combined in a specially designed mixer where the dispersed phase was introduced onto the wall of the pipe by use of a porous section. This minimised creation of dispersion at the mixer, so that any drops formed were created by turbulence and mixing within the pipe. Downstream of the test section, a separator equipped with knit-mesh cartridges was used to separate the two phases. Each phase was then returned by gravity feed to the storage tanks.

The test sections used were placed as far away from the mixer as possible in order to allow maximum flow development. The total height of the vertical section was 4 m while the distance from the mixer to the test section for the horizontal geometry was 4.5 m.

3.2. Drop sizing instrumentation

To obtain drop size distributions from the dispersions created in the pipeline, two optical techniques were applied. The first technique is based on laser backscatter and employed a Par-Tec 300C instrument manufactured by Lasentec™. The system comprises of a robust probe, which is inserted into the pipeline at 45° to the flow. A laser diode is situated within the probe and the laser light passes through an eccentric-rotating lens, which produces a circular rotating beam. This

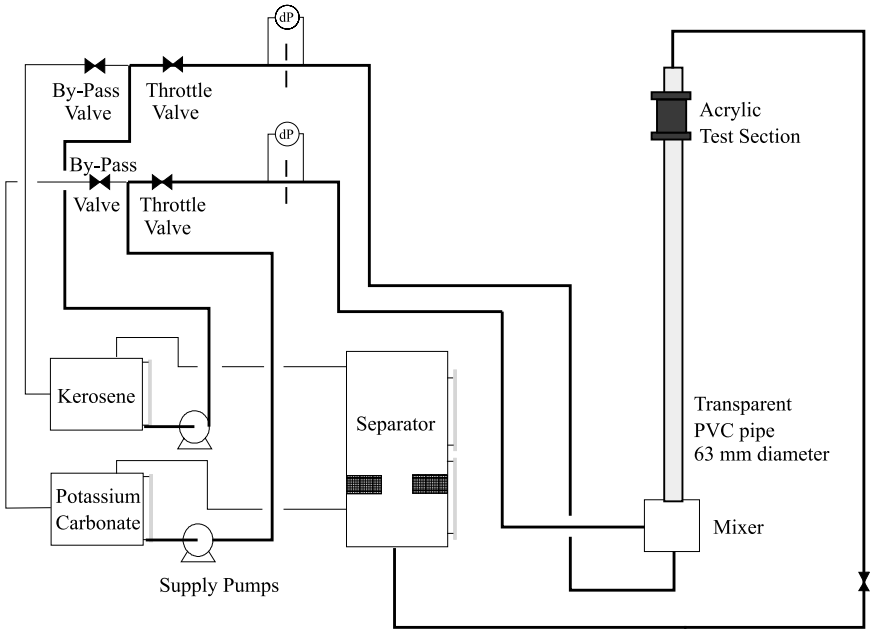

Fig. 1. Diagram of liquid–liquid flow facility.

Table 2
Physical properties of the fluids used

Aqueous phase viscosity (kg/ms)	Aqueous phase density $(kg/m)^3$
0.0016	1166

beam passes through a sapphire window and is focused at a certain distance into the flow. When this beam intercepts a droplet, the light is back scattered through the window and detected within the probe. The probability of the beam hitting any part of the drop is equal, so the instrument produces measurements of droplet chord lengths rather than diameters. The proprietary software produces distributions of droplet chord lengths for 38 logarithmic size bins from 1.8 to 1000 μm. The operation of a similar version of this instrument has been described in detail by Hobbel et al. (1991). To convert the chord length distributions produced by this technique to diameter distributions, a finite element method was utilised as described by Simmons et al. (1999).

The second technique used is also laser based and utilises Fraunhofer diffraction to determine droplet diameter distribution. The Malvern Instruments 2600 particle sizer employed illuminates the droplets with a low power collimated He–Ne laser beam. The scattered light passes through a Fourier transform lens and the far field diffraction pattern is focused onto a series of concentric photoelectric detectors. The diameter distribution is then determined from the scattered light intensity using a computer. The size range of this instrument is dependent upon the focal length of the Fourier lens used and hence varies with application. In these studies a 1000 mm lens was used which gives a size range of 18–1800 μm.

More information on the instrumentation used and the methods of deployment on the liquid–liquid flow facility are detailed in Simmons et al. (2000).

3.3. Flow conditions

Drop size and flow pattern data were taken for both horizontal and vertical upflow using the backscatter method for the first set of flow conditions in Table 3. Drop size distribution data was taken using both laser techniques at three positions in the pipe; at the centre-line and 7 mm either side. For horizontal flow, measurements were made at the centre-line and 7 mm above and below.

Both backscatter and diffraction measurement techniques were applied to the vertical test section for the second set of flow conditions. The choice of two different sets of flow conditions was necessary due to the different characteristics of the measuring techniques.

Flow patterns were determined for both geometries from high-speed video footage using a Kodak Ektapro camera at 1000 fps. A small quantity of fluorescent fluorescein sodium dye was added to the dispersed phase to aid the visualisation of droplet formation. Strong back illumination was used to determine the presence of droplets in both the water and kerosene layers. This was done to improve the accuracy of the flow pattern determination, as it can be difficult to distinguish between the D w/o +D o/w and Dw/o+w patterns. A summary is given in Tables 3 and 4.

Table 3
Flow conditions for drop data

Kerosene superficial velocity u_{so} (m/s)	Aqueous phase superficial velocity u_{sw} (m/s)	Mixture superficial velocity u_{mix} (m/s)	Dispersed phase concentration (% vol)	Horizontal flow pattern	Vertical flow pattern
(a) *Horizontal and vertical flow-back-scatter technique*					
0.837	0.158	0.995	15.9	SM	w/o
0.837	0.317	1.154	27.5	SM	w/o
0.837	0.488	1.325	36.8	*D* w/o +w	w/o
0.837	0.614	1.451	42.3	*D* w/o+w	w/o
1.49	0.158	1.648	9.6	*D* w/o+w	w/o
1.49	0.317	1.807	17.5	*D* w/o+w	w/o
1.49	0.488	1.978	24.7	*D* w/o+w	w/o
1.49	0.614	2.104	29.2	*D* w/o+w	w/o
2.393	0.158	2.551	6.2	w/o	w/o
2.393	0.317	2.710	11.7	w/o	w/o
2.393	0.488	2.881	16.9	*D* w/o+w	w/o
2.393	0.614	3.007	20.4	w/o	w/o
(b) *Back-scatter and diffraction techniques, upflow*					
0.837	0.029	0.866	3.3		w/o
1.49	0.029	1.519	1.9		w/o
1.837	0.029	1.902	1.5		w/o
2.393	0.029	2.422	1.2		w/o

Table 4
Flow observations for horizontal stratified flow configurations[a]

u_{so} (m/s)	u_{sw} (m/s)	Re_o (−)	Re_w (−)	h/D (−)
0.84	0.158	25515	21182	0.28
0.84	0.317	25913	39400	0.32
0.84	0.488	26203	58265	0.34
0.84	0.614	29771	55953	0.53
1.49	0.158	44664	23258	0.24
1.49	0.317	45346	36720	0.28
1.49	0.488	46517	56073	0.33
1.49	0.614	47920	68038	0.39
1.49	0.880	48892	91309	0.42

[a] SW, SW+MI, *D* w/o +w.

4. Discussion

The flow patterns observed for horizontal flow are sketched in Fig. 2 and compared to the flow pattern map of Trallero (1995) in Fig. 3. Dispersed flows were observed for the range of flow rates used for vertical upflow. The flow patterns obtained for horizontal flow were stratified with interface mixing, ST+MI; a continuous dispersion of water in oil with a water layer, *D* w/o +w; and a dispersion of water in oil, *D* w/o. A summary of the flow patterns observed is also shown in Table 2. Trallero (1995) defines a double dispersion, i.e. *D* w/o+*D* o/w, but no oil droplets could be observed in the water layer for this system. All the measured points lie to the right of the equal velocity (EV) boundary, where the actual velocities of each phase are equal, so for all cases the actual oil velocity is greater than that of the aqueous phase. The oil phase also occupies most of the pipe and for these reasons the dominant flow pattern is oil phase continuous, either with dispersion of water or a water layer present. The transition from ST+MI to *D* w/o+w is reasonably well predicted by the flow pattern map, but the transition to a complete dispersion of *D* w/o is overpredicted. The model uses a modified version of the breakage models of Hinze (1955) and Levich (1962). A correction factor is introduced which is a function of the dispersed phase concentration, ϕ,

$$f(\phi) = n\phi^m. \tag{13}$$

This factor includes empirical constants, m and n, which do not seem to correlate well for this flow system. Moreover, it does not reduce to unity at the limits of concentration.

To describe the drop size distribution, an upper-limit log-normal distribution (ULLN) was fitted to the backscatter data. This is illustrated on Figs. 4 and 5 which shows data taken at the centre line. The numbers in the legend are mixture velocities. Normalising the experimental data by the Sauter mean diameter reduces the data to one curve. The constants of the upper limit log-normal distribution were $\delta = 0.61$ and $a = 1.35$. This is a significant deviation from the values of $a = 1.2$ and $\delta = 0.9$ suggested by Karabelas (1978).

The Sauter mean diameters measured by the backscatter technique for horizontal flow are shown in Fig. 6. The open symbols denote measurements taken in the *D* w/o+w regime. The closed symbols are for measurements taken for a dispersion of water in oil (D w/o). At low

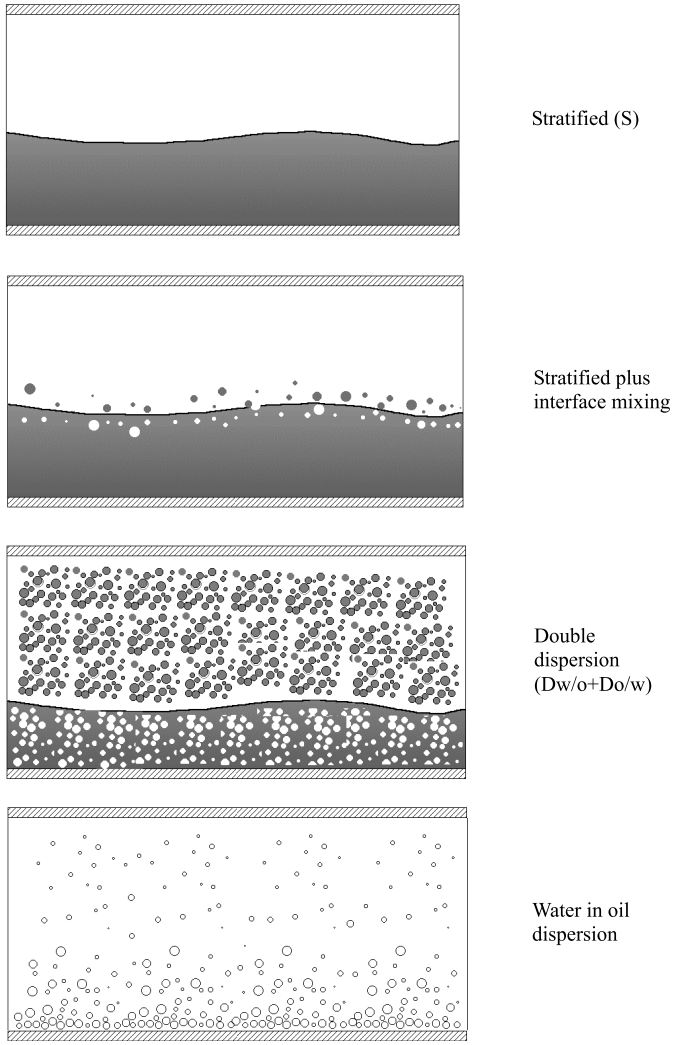

Fig. 2. Flow pattern classification.

velocities, the Sauter mean diameter is seen to drop at higher measurement positions. This is due to stratification of the drops in the dispersed layer at low flow rates, where few droplets are being formed from the liquid–liquid interface. At high velocities, the values converge. Much less variation with position is seen for vertical flow (Fig. 7), which is consistent with the observation of a homogeneous w/o dispersion at all the mixture velocities investigated.

A difficulty experienced was the different concentration ranges over which the optical techniques can operate. It was found that an insufficient number of drops were detected by the backscatter technique to give a statistically reliable distribution below concentrations of about 5% by volume. A similar problem was also reported by Hobbel et al. (1991). Conversely, the diffraction technique can only be applied at very low concentrations (below 3% v/v) due to

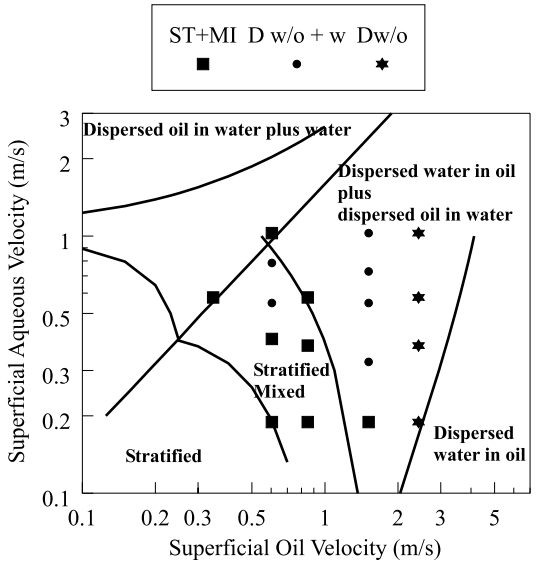

Fig. 3. Observed flow patterns for horizontal flow compared with flow map of Trallero (1995).

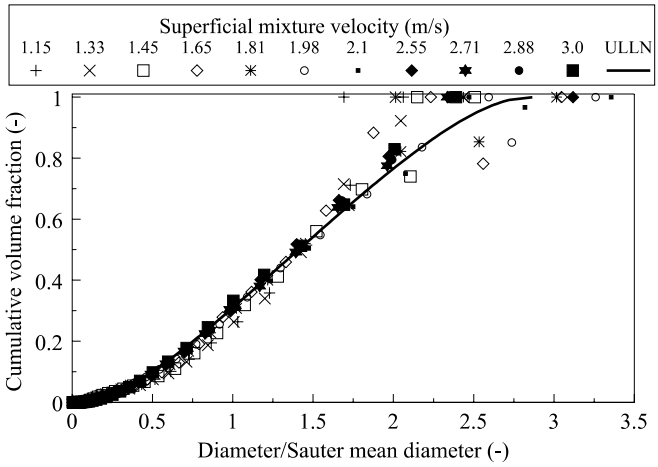

Fig. 4. Fitting ULLN distribution to the backscatter data for vertical flow.

limitations on flow turbidity. The theory of operation of the instrument assumes that the laser light is only scattered once by the drops. At high dispersed phase concentrations, multiple scattering occurs and the results obtained from the instrument can no longer be considered as reliable. To overcome this, two separate flow ranges were used so that the concentration was kept in the correct region. Fig. 8 compares the Sauter mean diameter values at the centre line measurement point for both backscatter and diffraction techniques for vertical upflow. The values of d_{32} are much lower for the low concentration measurements, made by the diffraction technique, than for

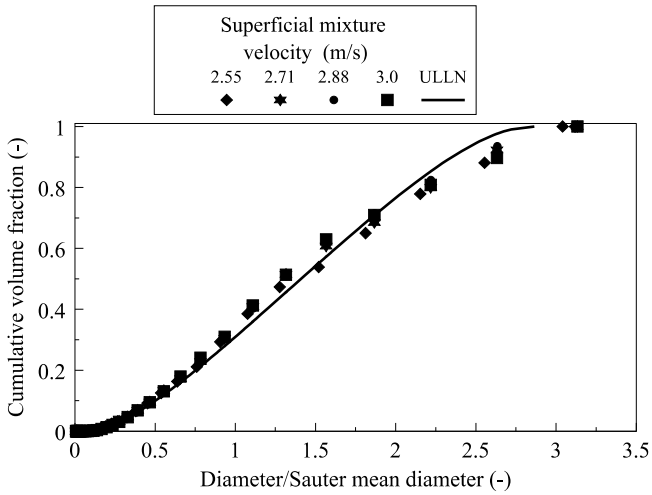

Fig. 5. Fitting ULLN distribution to the backscatter data for horizontal flow.

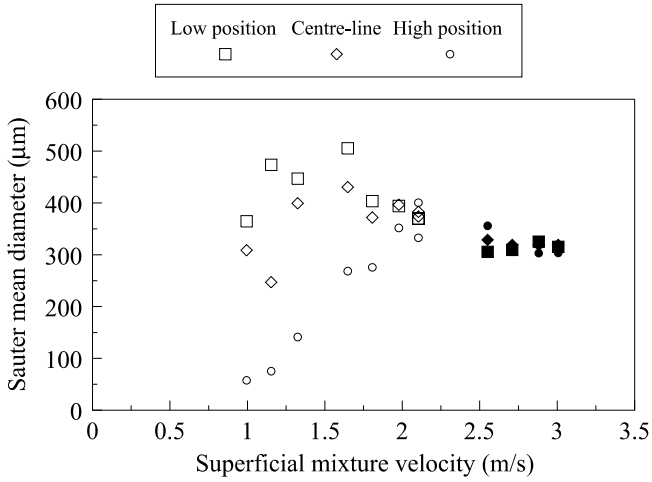

Fig. 6. Comparing data from the backscatter technique with measurement position-horizontal geometry.

the high concentration measurements made by the backscatter technique, they also decrease more rapidly with mixture velocity.

A maximum droplet size, d_{max}, can be inferred from the experimental data by use of the ULLN distribution, Eq. (12). The values of d_{max} obtained at low concentrations are compared with the model of Hinze (1955) calculated using Eq. (7) in Figs. 9 and 10. There is good agreement between the data and the model. This approach is extended to include the previous work shown in Table 1. All these data were obtained at low dispersed phase concentrations, and d_{max} was measured for all cases apart from the data of El-Hamouz et al. (1995). Here the relationship from Eq. (12) was again assumed. The experimental values are compared with the values calculated from Hinze

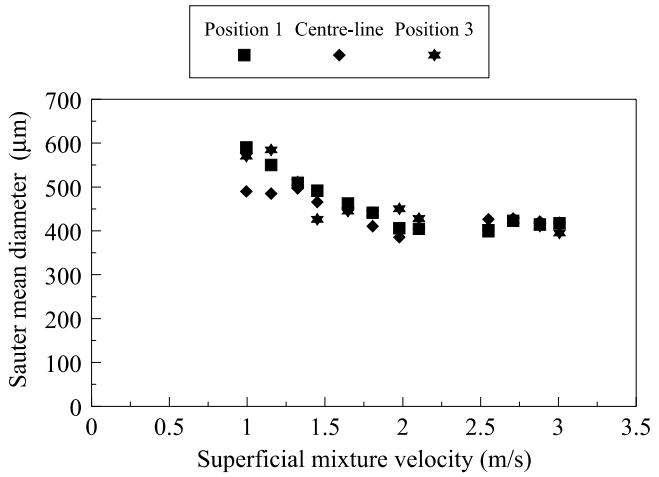

Fig. 7. Comparing data from the backscatter technique with measurement position-vertical geometry.

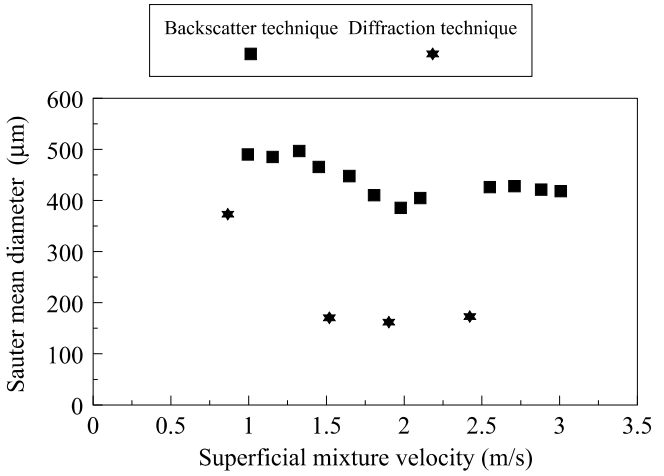

Fig. 8. Comparing data from both measurement techniques at the centre-line for the vertical geometry.

(1955), Eq. (7) and there is very good agreement, apart from the data of Karabelas (1978), measured for water droplets in kerosene, and the data of Kurban et al. (1995). Karabelas suggested that his measured drop sizes were biased to high values because of errors introduced by the sampling procedure. The sampling tube used in this work was located close to the bottom of the pipe. Therefore, it collected a disproportionate number of large drops, which may have coalesced near the pipe bottom. Kurban et al. (1995) is the only published paper where concentrations are not negligibly small.

Comparison with the high concentration data from the backscatter technique is made in Fig. 11. The values of d_{max} are underpredicted by the original theory of Hinze (1955) and the trend is also

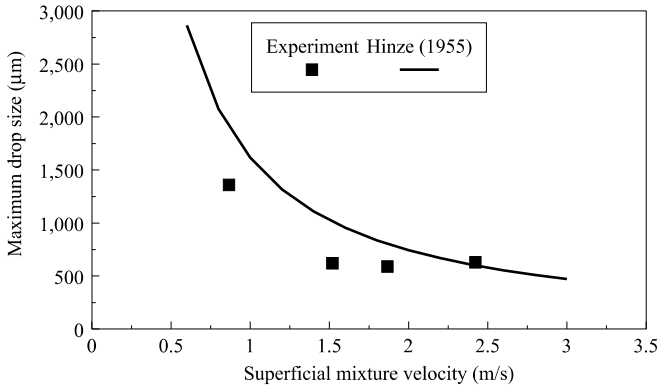

Fig. 9. Comparing vertical flow data obtained at low concentrations (diffraction technique) with the model of Hinze (1955), Eq. (7).

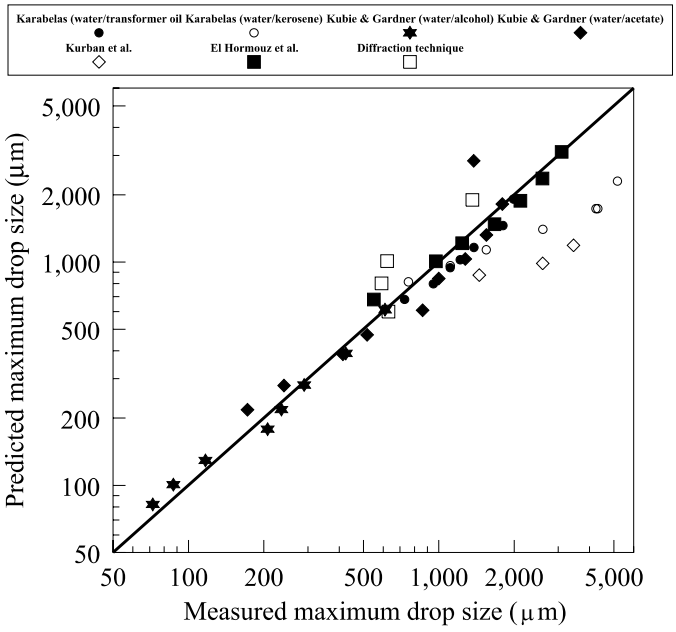

Fig. 10. Comparing measured values of d_{max} with the model of Hinze (1955), Eq. (7), for low concentration data from various workers.

steeper. The modified Hinze model proposed by Brauner (1999), Eq. (9) also does not describe the system adequately. The phenomenon of coalescence in the concentrated dispersions is not adequately modelled by either theory.

Angeli and Hewitt (2000) have observed an effect of pipe wall material on drop sizes. She shows results from hydrophilic (steel) and hydrophobic (plastic) pipes with the drop sizes from the former being smaller than those from the plastic pipe. The data from the steel pipe show good

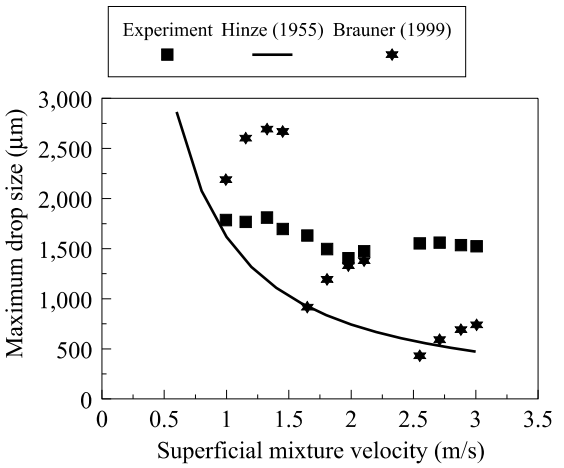

Fig. 11. Comparing vertical flow data obtained at high concentrations (backscatter technique) with the models of Hinze (1955), Eq. (7), and of Brauner (1999), Eq. (9).

agreement with the predictions from the model of Hinze (1955). However, the present low concentration data, which are from a plastic pipe, also agree with the Hinze predictions. Therefore it is suggested that the deviations seen above for higher concentration cases are not related to an effect of pipe wall material.

Central to the models described above are relationships between prime variables and the turbulence characteristics of the flow. Hinze (1955), considering dilute flows, reasonably employed relationships for single-phase flow. Brauner (1999) allowed for the presence of the dispersed phase, at other than negligible concentrations, by utilising the mixture velocity in her model. Examination of the measurements of Farrar and Bruun (1996) shows that, for a constant mixture velocity, the turbulence intensity rises from the single phase value to new value (10 times greater) beyond a critical concentration of about 5%. At higher concentrations, it is almost independent of concentration. Drop sizes remain almost constant below the critical concentration. Thereafter, they show a strong, direct relationship with concentration. However, it is possible that there is a reduction of turbulence for the present experiments. The main evidence for this comes from measurements made with other multiphase flows, e.g., by Tsuji et al. (1984) for gas/solids flows and by Azzopardi and Teixeira (1994) for annular gas/liquid flows. Tsuji et al. showed that there could be either augmentation or suppression of turbulence according to the particle size. Gore and Crowe (1989) using this and other data, showed that how the turbulence was affected depended on the ratio of particle size to turbulent length scale. When this ratio was >0.07 the turbulence intensity was increased. In contrast, for their annular gas/liquid flow data, Azzopardi and Teixeira found that even though their drop size/turbulent length scale was below the critical value, they were measuring turbulence intensities greater than the gas only values. A possible reason for this augmentation was the rough interface of the film on the pipe walls. However, Azzopardi and Teixeira showed that even when this was allowed for there was still augmentation. Azzopardi (1999) has suggested that the explanation for this apparent anomaly was due to newly created drops which, having been formed from the much slower liquid film, had lower initial velocities. For these drops the Reynolds number, $= \rho_g(u_g - u_d)d/\eta_g$, will have values large enough for there

to be production of extra turbulence by vortex shedding from these drops. Here ρ_g is the gas density, u_g the gas velocity, u_d the drop velocity, d the drop size and η_g is the gas viscosity. Liquid/liquid systems are expected to be nearer gas/solids flows than annular gas/liquid flows as there are no wall films present. For the present experiments the drop size/turbulent length scale ratio was determined to be 0.063. In calculating this, the turbulent length scale was taken as 0.11 the pipe diameter as proposed by Hutchinson et al. (1971). This value of the ratio implies a suppression of turbulence and from the model developed by Hinze (1955) larger sizes than predicted by Eq. (7) are expected. This is illustrated in Fig. 11. From Farrar and Bruun's data, the drop size/turbulent length scale ratio was found to be 0.29 and the expected augmentation of turbulence is reported.

5. Conclusions

Drop size distributions have been obtained for dispersions of an aqueous phase in kerosene for horizontal flow and vertical upflow using two optical measurement techniques. The drop size distributions obtained can be described by an upper limit log-normal distribution. For horizontal flow, stratification of the droplets was observed at low mixture velocities. For vertical upflow, homogenous dispersions were obtained and no stratification was observed.

Values of maximum drop diameter, d_{max}, obtained at low concentrations of the dispersed phase can be described by the theory of Hinze, which also applies to data obtained from other workers at low concentrations. Drop size distributions were also obtained at high dispersed phase concentrations; the backscatter technique employed in this study is one of the few techniques suitable for this task. However, the theory of Hinze cannot be applied to data taken at high concentrations. Further theoretical development of the physics of concentrated dispersions is necessary.

Acknowledgements

MJHS was supported by the University of Nottingham and BP Exploration. The flow facility was built under EPSRC grant GR/H43427. Thanks are also due to Prof. Neima Brauner for her valuable suggestions and discussion.

References

Angeli, P., Hewitt, G.F., 2000. Drop size distributions in horizontal oil–water dispersed flows. Chem. Eng. Sci. 55, 3133–3143.

Azzopardi, B.J., Teixeira, J.C.F., 1994. Detailed measurements of vertical annular two-phase flow – Part II: gas core turbulence. Trans. ASME J. Fluids Eng. 116, 796–800.

Azzopardi, B.J., Hibberd, S., 1994. Determination of maximum drop sizes in annular gas-liquid flow. In: Proceedings of the Sixth International Conference on Liquid Atomisation and Spray Systems, pp. 962–969.

Azzopardi, B.J., 1999. Turbulence modification in annular gas/liquid flow. Int. J. Multiphase Flow 25, 945–955.

Brauner, N., Moalem Maron, D., 1992a. Stability analysis of stratified liquid–liquid flow. Int. J. Multiphase Flow 18, 103–121.

Brauner, N., Moalem Maron, D., 1992b. Flow pattern transitions in two-phase liquid–liquid flow in horizontal tubes. Int. J. Multiphase Flow 18, 123–140.

Brauner, N., 1999. The prediction of dispersed flow boundaries in liquid–liquid and gas–liquid systems. 37th European Two Phase Flow Group Meeting Imperial College, London, 28–30 September, 1999.

El-Hamouz, A.M., Stewart, A.C., Davies, G.A., 1995. A study of kerosene–water dispersions in shear flow through pipes and fittings. In: Proceedings of the First International Symposium on Two-Phase Flow Modelling and Experimentation, pp. 987–997.

El-Hamouz, A.M., Stewart, A.C., 1996. On-line drop size distribution measurement of oil–water dispersion using a Par-Tec M300 laser back-scatter instrument. SPE Int. 36672, 1–14.

Farrar, B., Bruun, H.H., 1996. A computer based hot-film technique used for flow measurement in vertical kerosene–water pipe flow. Int. J. Multiphase Flow 22, 733–751.

Gore, R., Crowe, C.T., 1989. Effects of particle size on modulating turbulence intensity. Int. J. Multiphase Flow 15, 279–285.

Hinze, J., 1955. Fundamentals of the hydrodynamic mechanism of splitting in dispersion processes. AIChE J. 1, 289–295.

Hobbel, E.F., Davies, R., Rennie, F.W., Allen, T., Butler, L.E., Waters, E.R., Smith, J.T., Sylvester, R.W., 1991. Modern methods of on-line size analysis for particulate process streams. Part. Part. Syst. Charact. 8, 29–34.

Hutchinson, P., Hewitt, G.F., Dukler, A.E., 1971. Deposition of liquid or solid dispersion from turbulent gas streams: a stochastic model. Chem. Eng. Sci. 26, 419–439.

Karabelas, A.J., 1978. Droplet size spectra generated in turbulent pipe flow of dilute liquid/liquid dispersions. AIChE J. 24, 170–180.

Kubie, J., Gardner, G.C., 1977. Drop sizes and drop dispersion in straight horizontal tubes and in helical coils. Chem. Eng. Sci. 32, 195–202.

Kurban, A.P.A., Angeli, P.A., Mendes-Tatsis, M.A., Hewitt, G.F., 1995. Stratified and dispersed oil–water flows in horizontal pipes. In Seventh International Conference on Multiphase Production, Cannes, France, pp. 277–289.

Levich, V.G., 1962. Physiochemical Hydrodynamics. Prentice-Hall Inc, NJ.

Milne-Thomson, L.M., 1968. Theoretical Hydrodynamics, fifth ed. London, Macmillan.

Mugele, R.A., Evans, H.D., 1951. Droplet size distribution in sprays Ind. Engng. Chem. 43, 1317–1325.

Pacek, A.W., Nienow, A.W., 1997. Breakage of oil drops in a Kenics mixer, BHR 1997, Process Intensification.

Simmons, M.J.H., Langston, P.A., Burbidge, A.S., 1999. Particle and droplet size analysis from chord distributions. Powder Technol. 102, 75–83.

Simmons, M.J.H., Zaidi, S.H., Azzopardi, B.J., 2000. Comparison of laser based drop size measurement techniques and their application to dispersed liquid–liquid pipe flow. Opt. Eng. 39, 505–509.

Su, H., Hanzevack, E.L., 1988. A model for drop size distribution and maximum drop size in two-phase liquid–liquid flow. In: AIChE Annual Meeting, Washington, DC, 27 November–2 December 1988.

Trallero, J.L., 1995. Oil–water flow patterns in horizontal pipes. PhD Thesis, University of Tulsa.

Tsuji, Y., Morikawa, Y., Shiomi, H., 1984. LDV measurements of an air-solid two phase flow in a vertical pipe. J. Fluid Mech. 139, 417–434.

Valle, A., 1998. Multiphase pipeline flows in hydrocarbon recovery. Multiphase Sci. Technol. 10, 1–139.